Supplemental Material: Differentiating Contributions of Electrons and Phonons to the Thermoreflectance Spectra of Gold

Kexin Liu[1], Xinping Shi[1], Frank Angeles[1], Ramya Mohan[2],
Jon Gorchon[3], Sinisa Coh[1,2,a], Richard B. Wilson[1,2,b]

1) Mechanical Engineering, University of California, Riverside, CA, 92521, USA
2) Materials Science and Engineering, University of California, Riverside, CA, 92521, USA
3) Université de Lorraine, CNRS, IJL, F-54000 Nancy, France

a) sinisa.coh@gmail.com
b) rwilson@ucr.edu

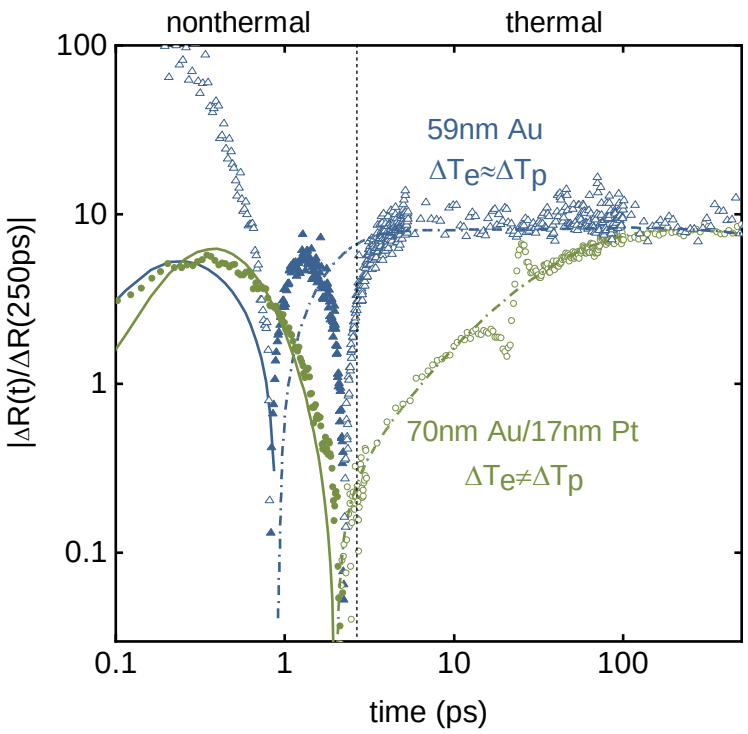

Supplementary Figure 1. Pump/probe data for Au and Au/Pt bilayer. Data is from a measurement with a pump wavelength of 900 nm, and a probe wavelength of 450 nm. Solid makers denote positive change in Au reflectance, while open markers are negative. The lines are the prediction of a two-temperature model as described in the main-text and below. We hypothesize that, at time scales less than 2 ps, the model predictions for the 59 nm Au film disagree with the data due to nonthermal effects and/or the effect of an acoustic strain wave. On timescales longer than 2 ps, electrons and phonons in the 60 nm Au layer are in equilibrium, and their contribution to the thermoreflectance signal cannot be differentiated. We overcome this obstacle by focusing our study on Au/Pt bilayers. In Au/Pt bilayers, the electron/phonon nonequilibrium persists for ~ 100 ps. The deviation between the model predictions and thermoreflectance data for the Pt/Au bilayer at ~30 ps is due to a longitudinal acoustic strain wave, which we use to measure the Pt and Au film thickness.

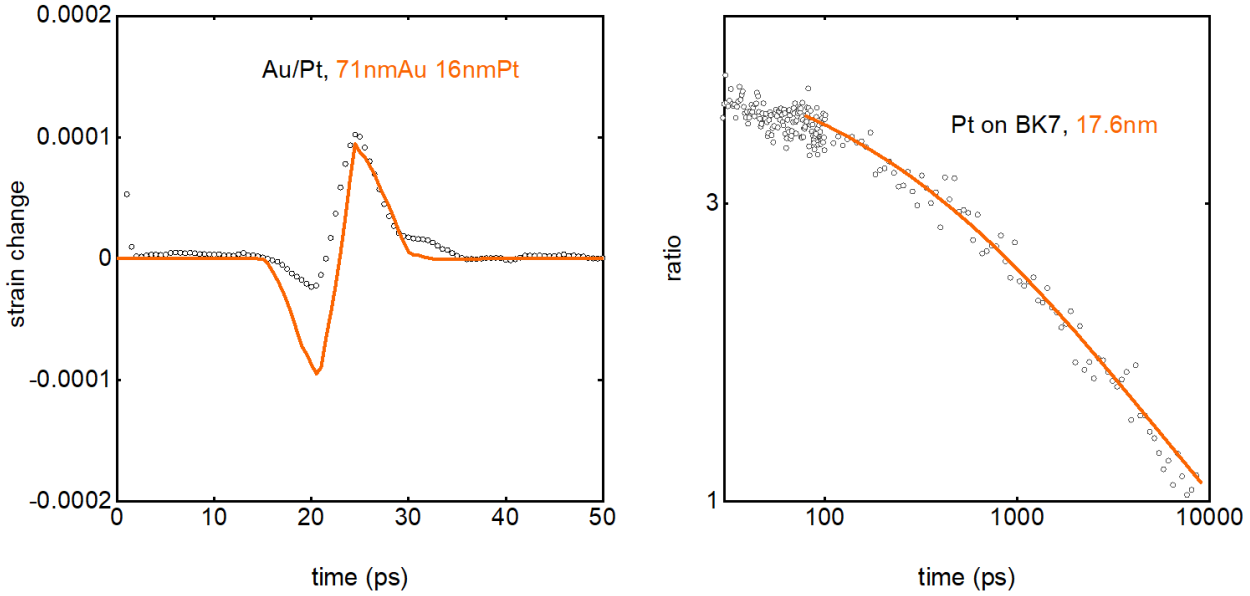

Supplemental Figure 2. (a) Picosecond acoustic data and acoustic model predictions. The picosecond acoustic data is arrived at by subtracting the thermal signal from our pump/probe data. We deduce the thickness of the layers by treating the Au and Pt thickness as fit parameters in the acoustic model. (b) TDTR measurement of a Pt film deposited on BK7 substrate with the same conditions as the Pt layer in the Au/Pt bilayer shown in (a). The line is a best fit to the data with a thermal model. We treated the Pt thickness as a fit parameter in the thermal model. We set the Pt film thickness for this bilayer to 16.8 nm, the average of the best-fit values in (a) and (b).

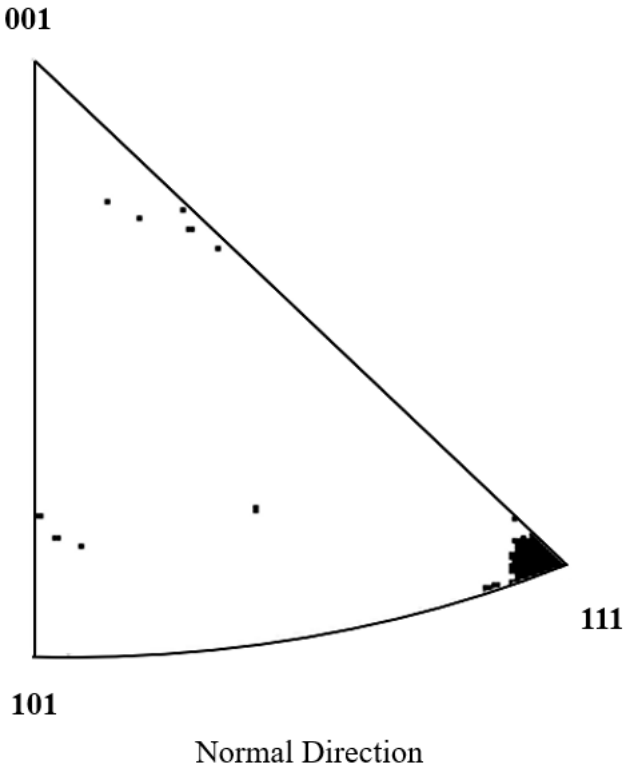

Supplemental Figure 3. A scatter plot of the EBSD Inverse Pole Figure of an Au/Pt/Sapphire film in the normal direction (thickness of Au layer ~70 nm). The data shows sharp crystalline texture in the [111] direction.

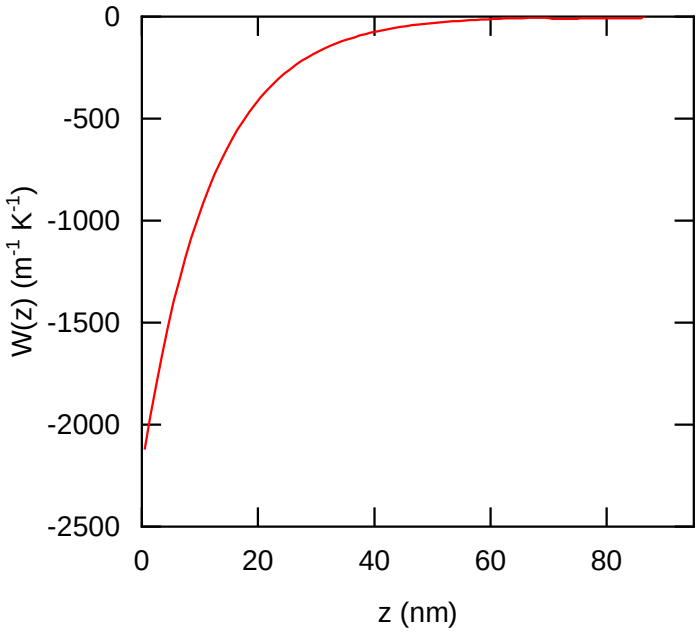

Supplementary Figure 4. Depth sensitivity of the thermoreflectance measurement of 70nm Au / 17nm Pt at a probe wavelength of 960 nm. We calculate the depth sensitivity using a multilayer reflectivity calculation [S1] and the thermo-optic coefficients for Pt and Au reported in Ref. [S2]. The area under the red line is the total thermoreflectance coefficient of the sample at a wavelength of 960 nm.

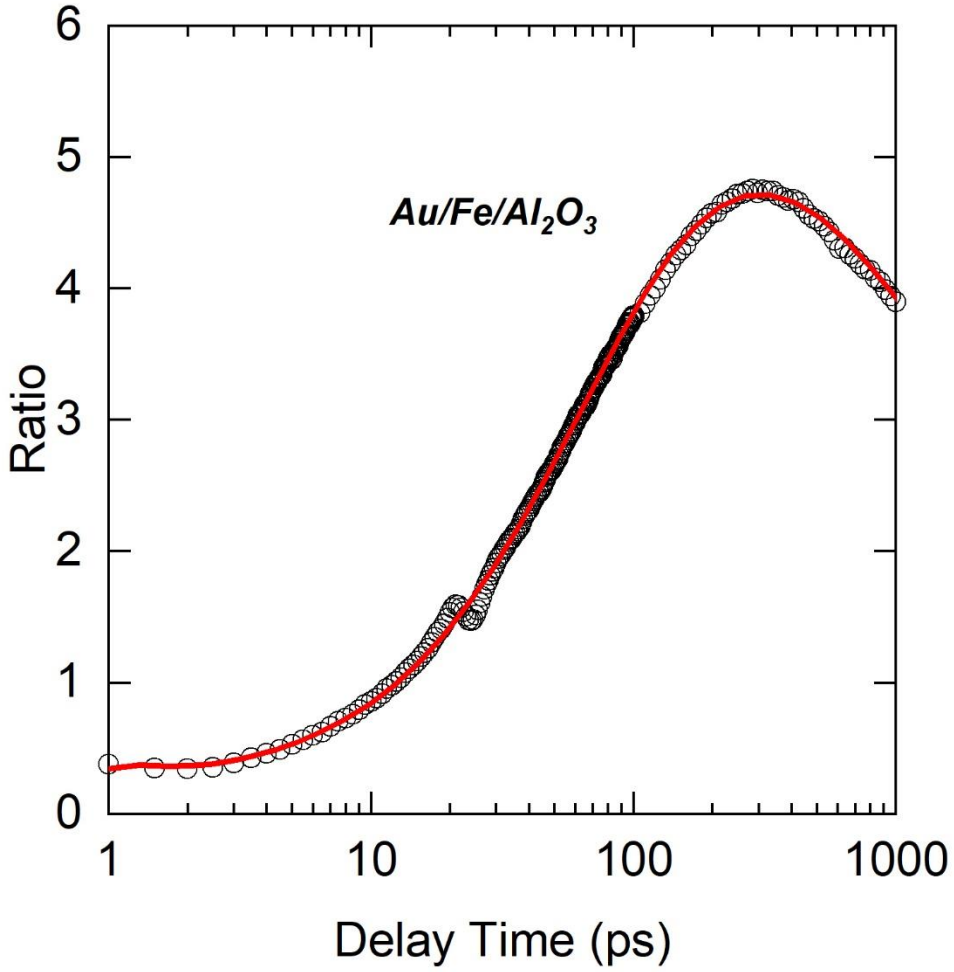

Supplementary Figure 5. Pump/probe data for a 73nm Au/ 18nm Fe bilayer sample. The data is proportional to change in reflectance of the Au at a wavelength of 783nm as function of pump probe time-delay. Lines are thermal model predictions for the change in reflectance with $|a| \approx 0.01$ and $|b| \approx 0.99$. The thermal model uses the following values for the thermal properties of Fe. An electron-phonon coupling parameter for Fe of 10^{18} W m^{-3} K^{-1}. A phonon heat-capacity of 3.5 MJ m^{-3} K^{-1}. An electron thermal conductivity (based on electrical resistivity measurements and WF-law) of 15 W m^{-1} K^{-1}. A phonon thermal conductivity of 10 W m^{-1} K^{-1} (based on TDTR measurements of the total thermal conductivity for a separately prepared 200nm thick Fe film, and the WF-law prediction for total thermal conductivity.) An electronic heat-capacity of 0.02 MJ m^{-3} K^{-1}.

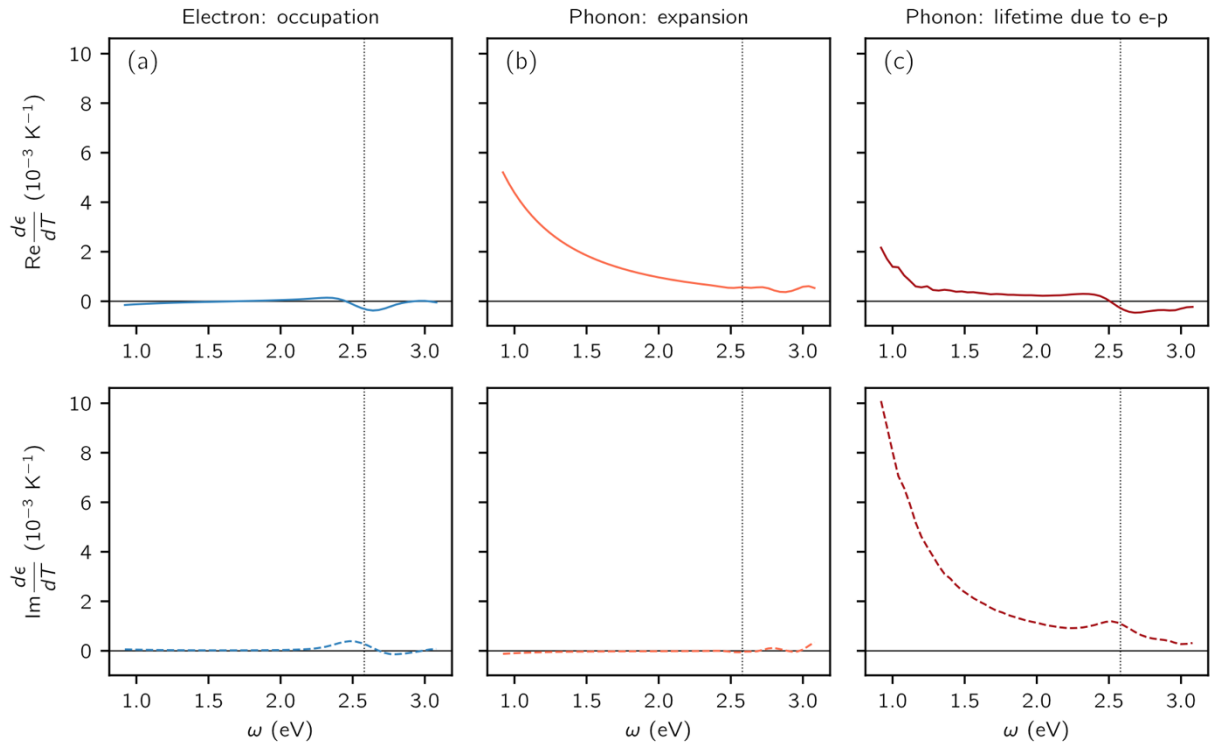

Supplementary Figure 6. Decomposition of calculated derivative of dielectric constant with respect to temperature as a function of photon energy. Top row shows the real part of the derivative, bottom row shows the imaginary part. Three columns correspond to contributions for the electron occupation, volume expansion, and thermal displacement of the atoms. The main effect of thermal displacement of the atoms is a change in the lifetime of carriers due to electron-phonon interactions.

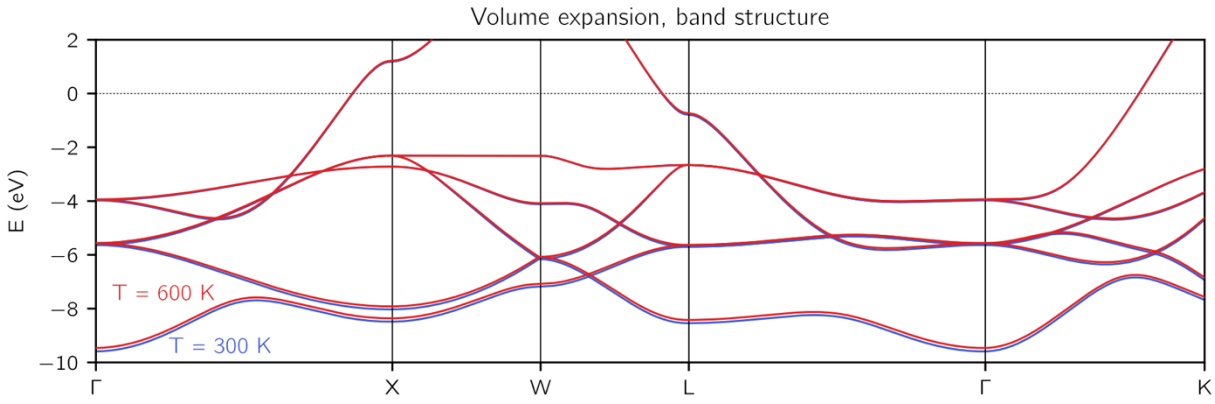

Supplementary Figure 7. Band structure of gold along high-symmetry path in the Brillouin zone for unit-cell volume at temperature of 300 K (blue) and 600 K (red).

Sample Growth and Characterization

The base pressure of the chamber was less than 4 x 10^{-7} torr prior to sputtering. During sputtering, the pressure was increased to 3.5 mTorr by introducing ultra-high purity Argon with a mass flow controller. We sputtered Pt and Au films from 1" and 2" inch targets at powers of 10 and 100 W, respectively.

Analysis of experimental data requires accurate measures of the Pt and Au film thicknesses. We use picosecond acoustics to measure the film thicknesses, see Supplementary Figure 2a. To further reduce uncertainty in the layer thickness, we also carefully calibrated the sputter deposition rates of the Au and Pt targets in the following manner. Before (after) deposition of the Au/Pt bilayer, we sputtered separate single-layer Au (Pt) films with conditions and times identical to those for the Au/Pt bilayers. We then used TDTR to determine the thicknesses of the Au and Pt single-layer samples by fitting the data with a thermal model whose only unknown parameter is film thickness, see Supplementary Figure 2b. These measurements of the "dummy" films gave thickness values within 10% of our estimates based on picosecond acoustic measurements of the bilayers themselves.

We measured the texture of the Au and Pt films with electron backscattering diffraction in a field-emission scanning electron microscope (Nova NanoSEM 450), equipped with an Oxford EBSD detector (NORDLYS Nano CCD Camera detector). We analyzed the EBSD maps and generated inverse pole figures (IPF) using the Oxford Instruments AztecSynergy software. Based on the scatter plots of the IPF in the normal direction, we find the film is highly textured in the [111] direction, see supplementary figure 3. We use the texture to estimate the speed of sound. The longitudinal speeds of sound in Pt and Au films in the [111] direction are 4280 and 3450 m/s, respectively.

Depth Sensitivity of Thermoreflectance Signals

Our experiments measure the temperature induced change of a sample's reflectance. In general, the change in reflectance of a sample will be a measure of the temperature-profile as a function of depth,

$$\Delta R(t) = \int_0^\infty \left[W_e(z)\Delta T_e(z) + W_p(z)\Delta T_p(z) \right] dz \,. \qquad \text{(S3)}$$

Here, W_e and W_p are weight functions that determines the sensitivity of the thermoreflectance to the change in electron and phonon temperatures ΔT_e and ΔT_p. When electrons and phonons are in equilibrium, Eq. (S3) simplifies to

$$\Delta R(t) = \int_0^\infty W(z)\Delta T(z)dz\,. \qquad \text{(S4)}$$

The weight functions decrease with increasing depth due to the finite optical penetration depth of light into metals.

To numerically calculate $W(z)$, we discretize the multilayer stack into 0.5 nm thick nodes. In other words, instead of performing a multilayer reflectivity calculation on a two layer system of air /70nm Au / 17nm Pt / sapphire, we perform the multilayer reflectivity calculation on a 177 layer system of air/[0.5nm Au]×140 / [0.5nm Pt]×34 / sapphire. The reflectivity of this system is defined as R_0. Then, to determine $W(z)$ at a specific depth $z0$, we modify the index of refraction of the node at depth z_0 from $n+ik$ to $\left(n+\frac{dn}{dT}(1K)\right)+i\left(k+\frac{dk}{dT}(1K)\right)$, and perform another multilayer reflectivity calcultaion. We define the reflectance of the modified system to be $R(z_0)$. Then, $W(z=z_0)=R_0-R(z_0)$. We repeat this for all 177 layers to derive $W(z)$ at all depths.

Calculation of the electron and phonon weight functions for our samples, W_e and W_p, requires knowledge of $\partial n/\partial T_e$ and $\partial k/dT_p$ for both Au and Pt, which we do not have. Alternatively, calculation of the weight function $W(z)$ requires only knowledge dn/dT and dk/dT for Au and Pt. We use the data reported in Ref. [S2] to calculate $W(z)$ for a (70nm Au)/(17nm Pt)/sapphire sample as a function of wavelength. We show an example plot for $W(z)$ at a wavelength of 960 nm in Supplemental Figure 4. Then, to analyze our data, we assume that $W_e(z)=a(\lambda)W(z)$ and $W_p(z)=b(\lambda)W(z)$. We then use Eq. (S3) and our two-temperature model predictions to calculate $\Delta R(t)$.

Supplementary References

S1. Hecht, E., *Hecht optics.* Addison Wesley, 1998. **997**: p. 213-214.

S2. Wilson, R., B.A. Apgar, L.W. Martin, and D.G. Cahill, *Thermoreflectance of metal transducers for optical pump-probe studies of thermal properties.* Optics express, 2012. **20**(27): p. 28829-28838.